http://ansinet.com/itj

ITJ

ISSN 1812-5638

INFORMATION TECHNOLOGY JOURNAL

ANSInet
Asian Network for Scientific Information
308 Lasani Town, Sargodha Road, Faisalabad - Pakistan

Information Technology Journal 5 (4): 719-725, 2006
ISSN 1812-5638

Radiation Spectral Integral for Tapered Structure in Optical Communication

[1]A. Temmar and [2]A. Belghoraf
[1]Institute of Telecommunications of Oran, Algeria
[2]Institute of Electronics, University of Sciences and Technology of Oran, Algeria

Abstract: The study here is mainly adapted to the implementation of a radiation spectral integral, involved to describe modal field behaviour outside a non uniform structure for optical communication purposes. This is achieved by simply associating with each individual spectral plane wave incident on any boundary of the structure, a refracted wave with appropriate transmission coefficient. This spectral integral describes rigorously and systematically a source-free field behaviour not only before and after a branch point singularity (transition region), but also outside a tapered structure too. In this sense, the implementation of the resulting spectral formulation, for the case of homogenous media, contains all informations pertinent to the modal propagation mechanism, not only outside the structure, but also inside it, before and after the singularity caused by cut off of the propagating mode.

Key words: Integrated Optics, optical communication, thin film waveguide, fiber optics

INTRODUCTION

As the purpose of this study is an original investigation of a structure using a tapered configuration; the impetus was given in order to analyse the field distribution involved in the propagation process outside such a structure using the tapered waveguide as a main body (Arnold, 1985). It is then, necessary to track the motion of any observation point $\underline{X}$, not only along and inside the tapered waveguide itself, but also across the cross section of its adjacent bottom medium (n_2). The observation point $\underline{X}$ is locally positioned at a thickness T, as shown in Fig. 1.

From a physical point of view, rays of the spectrum undergo bottom reflections at Γ_{12} interface adjoinning the wedge angle a and at vicinity of the critical angle θ_c defined by the relation cos (θc) = (n2/n1); when total internal reflections prevail. But, for observation points $\underline{X}$ located beyond critical transition range, rays reaching $\underline{X}$ begin to radiate through Γ_{12}. It is the purpose of this article to investigate the modal field distribution in the adjacent bottom medium (n_2). To achieve this, it will be necessary to introduce the concept of a radiation spectral integral which governs the field propagation in medium (n_2) and which will describe the radiation mechanism taking place in the structure. The following treatment could also apply to top adjacent medium (n_3) which is the free-space. But we restrict ourselves to the radiation process occuring at bottom medium (n_2) only; for one has appropriately chosen the refractives indices such as, n1>n2>n3.

MATERIALS AND METHODS

Model presentation: The mathematical model implementing the radiation integral in an open region can be presented by a spectral integral representation R(X,θ). This is accomplished by extending the preceeding plane wave spectral analysis fully expressed by Arnold (1985) and Belghoraf (1992), hence:

$$R(X,\theta)=(2a)^{-1/2}\int_c \exp[jkS(X,\theta)]d\theta \tag{1}$$

Where the integration contour (C) is fully developed by Belghoraf (1988). The phase S(X,θ) will explicitly be defined later. The wavenumber k in here refers to bottom medium ($k = n_2\ k_0$). The parameter k0 is the free-space wavenumber. The expression given by Eq. 1 must satisfy the boundary conditions at Γ_{12}. That is at X = 0 or X = a, respectively (Fig. 1). In this respect, one constructs the radiation integral R(X,θ) by tracking the spectrum of a particular and appropriate species of wave that radiates by refraction into the corresponding boundary and which satisfies that boundary condition. To present the radiation integral referred to bottom boundary Γ_{12}, we consider only one type of wave among the four species introduced by Arnold (1985) and Belghoraf (1992) and which is characterised by the phase $S_0^u(X,\theta)$. This choice is justified by the fact that $[ikS_0^u(X,\theta)]$ is a wave which is destined to be refracted at the bottom medium (n_2). Multiplying the appropriate downward propagating plane waves $S_0^u(X,\theta)$ in Eq. 1 by the transmission coefficient at

Corresponding Author: A. Temmar, Institute of Telecommunications, Rout d'Es-Senia, BP 1518 M'Nouer, Oran 31000, Algeria
Tel: (213)41594436-165 Fax: (213)41594418

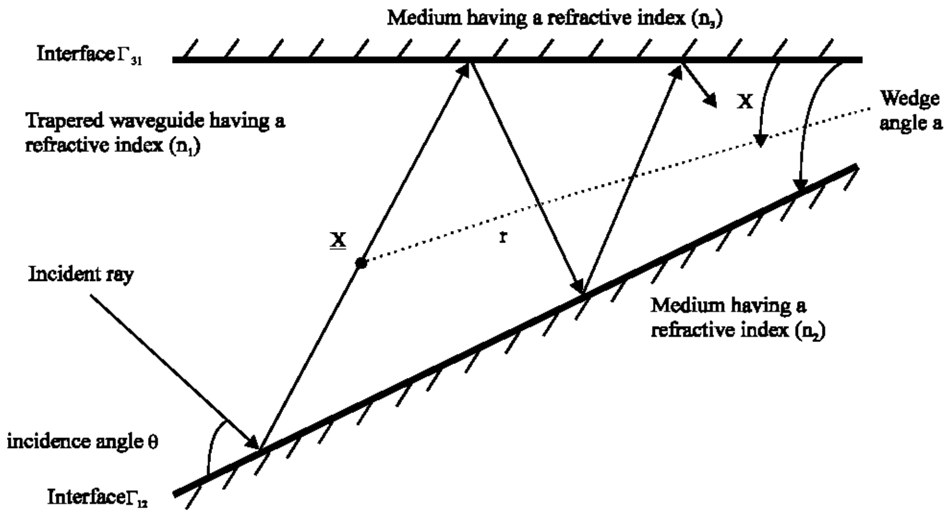

Fig. 1: Tapered waveguide under investigation. The observation point X≡(X,r) is positioned at a local thickness T

Γ_{12} interface, one obtains the radiation integral governing the field distribution in adjacent bottom medium (n2):

$$R(X,\theta)=(2a)^{-1/2}\int_{c}\{1+\exp[i\phi(\theta)]\}\exp\{i[-n_2 k_0 r\cos(\theta''-a+X)-1/2\phi(\theta)+[1(2a)]\int_{\theta_c}^{\theta}\phi(\theta')d'+[(\pi\theta)/(2a)]-(\pi\theta q)/a]\}d\theta \quad (2)$$

We bear in mind that $\phi(\theta)$ is the phase of the Fresnel reflection coefficient (Tamir, 1979) and q is the mode number to be exited along the structure. We also recall that the incidence angle θ becomes θ'' corresponding to the direction of propagation of the refracted wave in the adjacent bottom medium (n_2). These angles are both interrelated by snell's law, which stipulates that:

$$n_1\cos(\theta)=n_2\cos(\theta'') \quad (3)$$

Combining Eq. 2 and 3, after expanding the cosine term in the integrand of Eq. 2, we obtain after neglecting terms which vanish as $a\to 0$ (this is physically compatible with our structure geometry).

$$R(X,\theta)=(2a)^{-1/2}\int_{c}2\cos[\phi(\theta)/2]\exp[ikS(X,\theta)]d\theta \quad (4)$$

$$kS(X,\theta)=[1/(2a)]\int_{\theta_c}^{\theta}\phi(\theta')d\theta'-[\pi\theta/(2a)](2q-1)-[(k_0 n_2 r)/n_1][n_1\cos(\theta)\cos(X-a)-\sin(X-a)(n_2^2-n_1^2\cos^2(\theta))^{1/2}] \quad (5)$$

Parametric eigenvalue equation of the radiation spectral integral: To evaluate Eq. 4 asymptotically by means of saddle point method (Belghoraf, 1988), one ought to reconsider the new eigenvalue equation by finding zeroes (saddle point θ_q) of the derivative of the phase function in Eq. 5, one sets:

$$\frac{dS}{d\theta}(X,\theta_q)=0 \quad (6)$$

Combining Eq. 5 and 6, yields the new characteristic equation, which is:

$$\sin(\theta_q)\cos(X-a)+[\phi(\theta_q)-\pi(2q-1)]/[2rak_0n_2]+\sin(X-a)\frac{n_1\sin(\theta_q)\cos(\theta_q)}{(n_2^2-n_1^2\cos^2(\theta_q))^{\frac{1}{2}}}=0 \quad (7)$$

One notices the dissimilarity between Eq. 7 and the original eigenvalue equation treated (Arnold, 1985; Belghoraf, 1992). The former exploits the concept on an intrinsic field integral used to analyse field propagation inside the tapered waveguide; whereas the latter makes use of a concept of radiation integral developed to investigate the field behaviour outside the tapered waveguide. In Eq. 7 the additional terms are due to the X-dependence quantity which mathematically accounts for the dependence on depth in the adjacent bottom medium (n_2); and which appears here to behave as a parameter. At interface Γ_{12}, say at X = a, Eq. 7 and that found by Arnold (1985) and Belghoraf (1992) are identical. Hence, they engender the same saddle points θ_q. For at

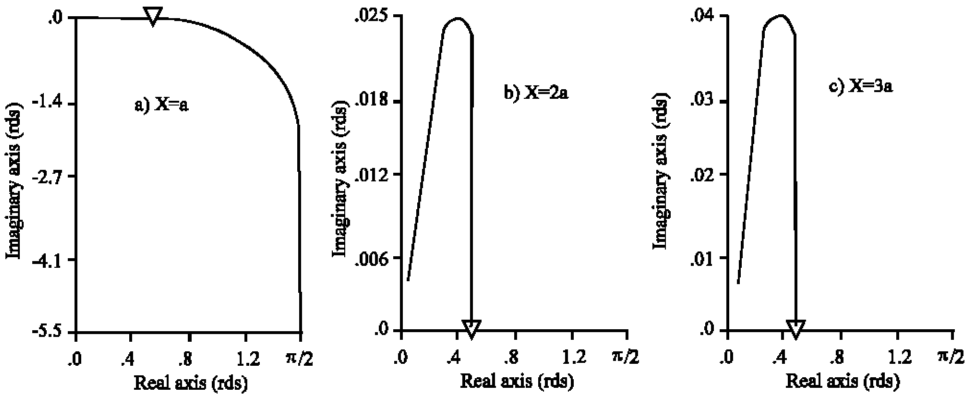

Fig. 2: Computation of eigenvalue equation Eq. 7 of the radiation integral. Solutions in the complex θ plane are the incident angle θ_q (saddle points) for the lowest mode, as the thickness T is arbitrary reduced. Three multiple values of the wedge angle a are considered for the cross variable X. the wedge angle a = 0.027 rds. The refractive indices in each medium are: $n_1 = 2$; $n_2 = 1.76$; $n_3 = 1$. The ∇ sign in figures locates the branch point θ_c

X = a, matching boundary values are necessarily required between the construction of the radiation integral R(X,θ) whose eigenvalue equation is given by Eq. 7 and that of the intrinsic integral I(X,θ) developed by Arnold (1985) and Belghoraf (1992) whose eigenvalue equation is also given there. One recalls that I(X,θ) describes the field inside the tapered waveguide and it is analytically expressed in the cited references. A proper substitution of φ(θ) in Eq. 7 by the phase of the Fresnel's coefficient leads to the corresponding eigenvalue equations which engenders the saddle points θ_q. The saddle points are then located for each observation point X defined by the polar coordinates X≡(X, r). The parametrically computed eigenvalue Eq. 7 is depicted in Fig. 2 for successive values of the transverse variable X (X≥a) and for the lowest mode only. In other words, Fig. 2 show the physical effect on the eigenvalue Eq. 7, of moving the observation point X outside the tapered waveguide and away from bottom boundary Γ_{12}. Figure 2a shows a plot corresponding to the parameter X = a, where the observation point is located on bottom interface Γ_{12}.

One notes that such a parametrical case has already been treated via the eigenvalue Eq. 7, whose numerical plotting is reported (Arnold, 1985; Belghoraf, 1992); a case dealing with the analysis inside the tapered optical waveguide. Locating an observation point X at X = 2a or at X = 3a, as shows by Fig. 2b and c, respectively, has the effect of shifting up the solutions of Eq. 7 (saddle points θ_q); particularly those lying beyond the transition region, to a region near the branch point θ_c which is denoted by ∇ sign in figures. For those solutions which are situated in the guided wave region (region delimitted by θ<θc), they exhibit a slight positive imaginary component. In the case (X = 2a or X = 3a), all solutions which are supposed to belong to the leaky wave region (region delimitted by $\theta>\theta_c$), seem to be coinciding with the branch point θ_c In other words, choosing a thickness T beyond transition region, will have the effect of bringing all complex saddle points to coalesce with θ_c Such an effect, exhibited by Fig. 2b and c, can geometrically be explained by reference to Fig. 3. As a matter of fact, in the guided wave region, as in Fig. 3a, the saddle points θ_q are within the interval $0<\theta_q<\theta_c$. Consequently, all rays inside the tapered waveguide undergo total multiple reflections at Γ_{12} and Γ_{31} interfaces. For any observation point X located outside the tapered waveguide and within the guided wave region; there are evanescent waves accommodate by the complex θ_q.As X moves away from Γ_{12} interface (as X increases), the transverse propagation constant τ of that evanescent wave becomes 'more complex' and entails a strongly decaying evanescent field. The constant τ is defined as follows:

$$\tau = (n_2^2 - n_1^2 \cos^2(\theta q))^{1/2} \tag{8}$$

Hence, one expects the imaginary part of the saddle point to increase. However, in the leaky wave region in contrast, Fig. 3b shows how the rays are refracted into medium (n_2), once the branch point θ_c is exceeded by θ_q. In this case, any observation point X outside the tapered waveguide receives the contribution of 2 distinct rays impinging at Γ_{12} interface, from 2 angles of incidence, θ_{q1} and θ_{q2}. Therefore, 2 saddle points (θ_{q1} and θ_{q2}) are required at a given thickness T and at a given transverse variable X (X>a). Because, one of these is at incidence

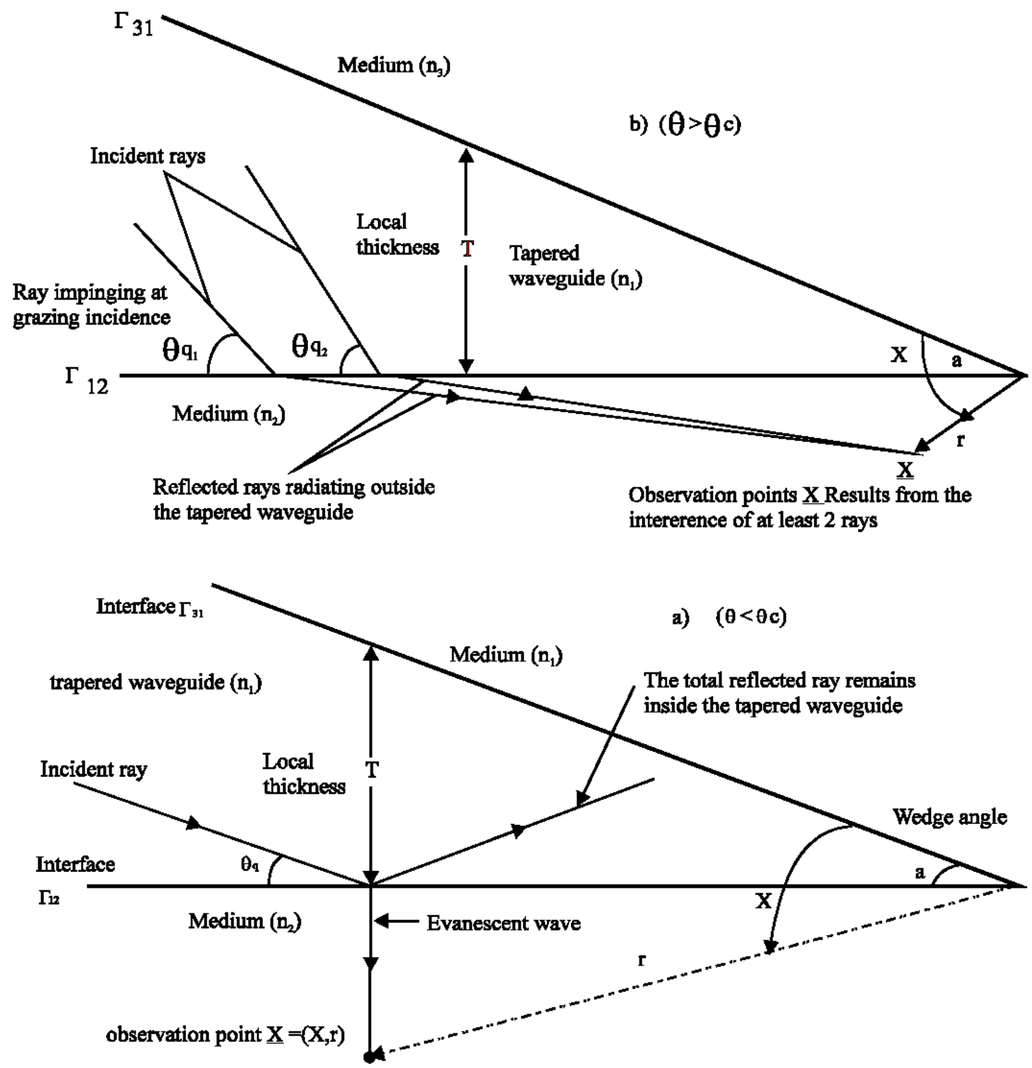

Fig. 3: Geometrical configuration of rays outside the tapered optical waveguide. a) Observation point X located in the guided wave region ($\theta<\theta_c$). b) Observation point X located beyond the transition region ($\theta>\theta_c$)

angle near to θ_c; the corresponding ray refracts from the tapered waveguide to the open medium (n_2), with a near grazing refraction angle. As the saddle point is condensed near the singularity θ_c, it is very difficult (if not impossible) to numerically assess absolutely the branch cut contribution. Such an effect, which manifests itself strongly when the observation point X is located outside the tapered waveguide (X>a) and beyond transition region, complicates the evaluation of the integral $R(X,\theta)$ in Eq. 4 by the saddle point method.

RESULTS AND DISCUSSION

Integrand variation of the radiation integral along the real axis: To circumvent those above difficulties and to achieve integration of Eq. 4 systematically, we suggest another method, already used (Belghoraf, 1992); which is to keep the undeformed original contour (C) and to abandon the saddle point method. The original contour (C) has a path coinciding with the real axis. We omit however the two lower tails because computational results have shown that their evanescent contributions are negligible compared to the real axis integration. Hence, we shall restrict the integration contour (C) to the interval $0<\theta<\pi/2$. For justification, let us plot the variation of the phase $S(X,\theta)$ of the integrand in Eq. 4 along the real axis at a given observation point X situated on bottom boundary Γ_{12} (X = a). Only the lowest mode is concerned.

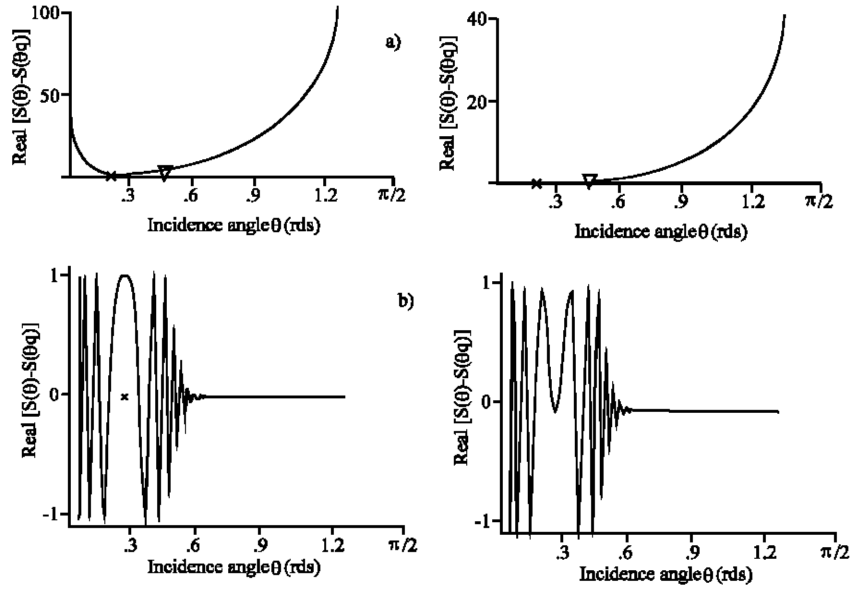

Fig. 4: a) Computation of the phase in the radiation integral Eq. 4, versus the incident angle θ varying along the ral axis. b) Computation of the integrand in the radiation integral Eq. 4 versus the incidence angle θ varying along the real axis. The saddle point θ_q is located in the guided wave region at k_0 T = 5. Mode 1, normalised critical thickness = 1.75. The x sign locates a saddle point θ_q; the ∇ sign locates the branch point θ_c.X = a = 0.027 rds

Saddle point θ_q located in the guided wave region: Figure 4a shows the complex variation of $S(X,\theta)$-$S(X,\theta_q)$ versus the incidence angle θ varying on the real axis. The real saddle point θ_q is located in the guided wave region at $k_0T = 5$. Real $[S(X,\theta)$-$S(X,\theta_q)]$ has an extremum at the chosen saddle point θ_q, which is denoted by the x sign in figures. Its imaginary part is zero for all Real θ's lying in the region $\theta<\theta_c$; where θ_c is the branch point for the phase $S(X,\theta)$ and it is denoted by ∇ sign in figures.

This means that Imag $[S(X,\theta)]$ is constant in the guided wave region. However when $\theta>\theta_c$, the imaginary part increases in magnitude, then leakage occurs. It is that very imaginary part of $S(X,\theta)$ that accounts for the amplitude decay of the field in the leaky wave region. In contrast, Real $[S(X,\theta)]$ decreases towards the constant Real $[S(X,\theta_q)]$ as θ tends to θ_q and increases as θ tends to θ_c and beyond. Figure 4b shows the complex variation of the integrand in Eq. 4, when the incidence angle θ varies on the real axis. Both components exhibit extrema at location of the saddle point. They oscillate initially, then decay exponentially as the incidence angle θ approaches $\pi/2$. This signifies that for $\theta>\pi/2$, the radiation integral of Eq. 4 engenders a vanishing field. In other words, there is no contribution of rays whose incidence angle is higher than $\pi/2$. This important statement justifies and accounts for the neglect of all types of subsequent rays in the establishment of Eq. 4.

Saddle point θ_q located in the leaky wave region: Figure 5a shows the same phenomena for a saddle point θ_q located in the leaky wave region at k_0 T = 1.2. We notice that $S(X,\theta)$-$S(X,\theta_q)$, accommodates a shift due to the fact that the saddle point θ_q is complex in this leaky wave region. Therefore, any variation of θ on the real axis, will never coincide with θ_q. Henceforth, $S(X,\theta)$-$S(X,\theta_q)$, will never fall to zero. This explains why $S(X,\theta)$-$S(X,\theta_q)$ exhibits a shift in its real part. This shift is more accentuated as θ_q becomes strongly complex; that is to say, as the observation point $\underline{X}$ tends towards the apex (or as T diminishes). As for the variation of the integrand of Eq. 4, Fig. 5b shows that initially it exhibits more rapid oscillation and then decays exponentially and faster than in Fig. 4b.

Hence, here too, the field engendered by the radiation integral Eq. 4 vanishes as θ tends towards $\pi/2$. For any location of the saddle point θ_q with respect to θ_c, it is safe to neglect the field contribution outside the range $0<\theta<\pi/2$. Returning to the radiation integral in Eq. 4, we shall then perform it along the real axis and in the interval $0<\theta<\pi/2$. In this case, the presence of any branch point will automatically be taken care off (Belghoraf, 2001). The convergence of Eq. 4 is, however, guaranteed by taking an integration step much smaller than the oscillating periods of Fig. 4 and 5. It is also necessary to maintain the same branch conventions for $(\theta-\theta_c)^{1/2}$ and $(\theta-\theta'_c)^{1/2}$,

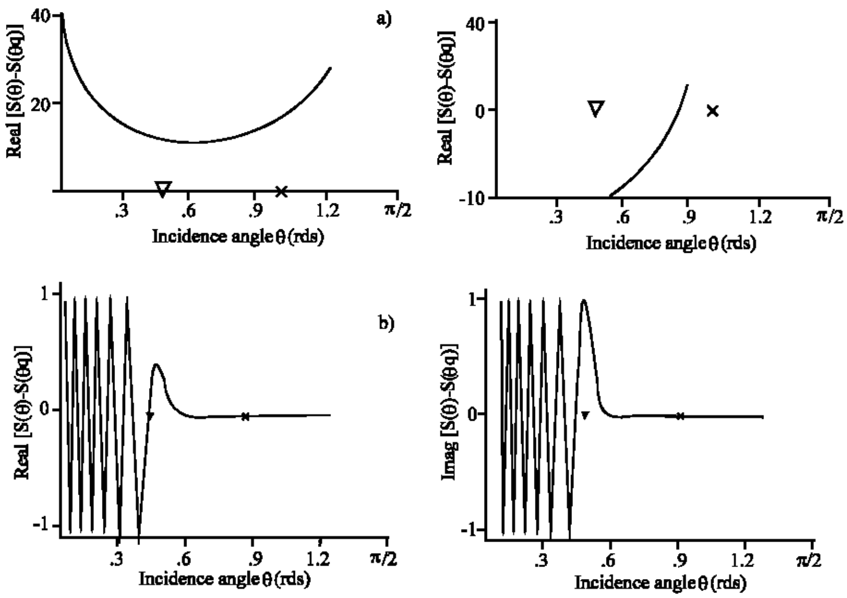

Fig. 5: a) Computation of the phase in the radiation integral Eq. 4, versus the incident angle θ varying along the ral axis. b) Computation of the integrand in the radiation integral Eq. 4 versus the incidence angle θ varying along the real axis. The saddle point θ_q is located beyond transition region (in leaky wave region) at k_0 T = 1.2. Mode 1, normalised critical thickness = 1.75. The x sign locates the saddle point θ_q; the ∇ sign locates the branch point θ_c. X = a = 0.027 rds. (n_1 = 2, n_2 = 1.76, n_3 = 1)

defined earlier. In as far as we are not using the saddle point method to calculate Eq. 4, knowledge of the saddle point θ_q is not necessary. In spite of this, we still represent each observation point $\underline{X}$ ≡ (X,r) by its equivalent notation $\underline{X}$ ≡ (X,θ_q). Note that Fig. 4 and 5 have all been numerically carried out for an observation point $\underline{X}$ at X = a and for the first mode q = 1 only. Similar qualitative results could have been obtained for any other parameter.

CONCLUSIONS

Numerical plotting of the radiation field in the guided wave region: Let us now concentrate first on Fig. 6. They shows the variation of the normalised field modulus in medium (n_2), versus the variation X, for mode 1.

Three locations of the observation point $\underline{X}$ are considered in the guided wave region, θ_q<θ_c They correspond to the three distinct normalised thicknesses in (i), (ii) and (iii) in figures 6 Thereby, it is clear that, as θ_q approaches θ_c (that is to say, as k_0 T approaches the critical thickness of the corresponding mode 1), the evanescent field decays less rapidly in the medium (n_2). The decay is more strongly evanescent, when $\underline{X}$ is located far from θ_c, as in (i), than when it is near, as in (iii). This is mainly because, in such a region, the waves inside the tapered waveguide are totally guided. When θ_q approaches θ_c, as in (iii), energy starts leaking out from the inside of the tapered waveguide to medium (n_2). As a matter of fact, this leakage near the transition region, makes the amplitude of the cross section field inside the tapered waveguide decrease in the guided wave region of course, the above remarks hold for any higher mode, characterised by its own corresponding critical thickness.

Numerical plotting of radiation field in the leaky wave region: In this case, all observation points $\underline{X}$ are located in the leaky wave region, such as θ_q >θ_c. In this region, energy is leaked out from the tapered waveguide to medium (n_2). Such a leakage characterises the radiation process taking place at bottom interface Γ_{12}. The light rays, then, are no longer totally reflected back into the tapered waveguide, but are partially transmited into medium (n_2) as refracted waves. Figure 7 show the variation of the normalised modulus of the radiated field, versus the angular variable X, for mode 1.

Each position of $\underline{X}$ is located in the leaky wave region. It is seen in each plotting that the field oscillates to a maximum, then decays exponentially because of the continuous refraction taking place in medium (n_2). Also, in each diagram, the locus engendered by each maximum of the radiated field describes a caustic (Oliver, 1974) whose gradient with respect to the bottom interface Γ_{12}, corresponding to X = a, represents the

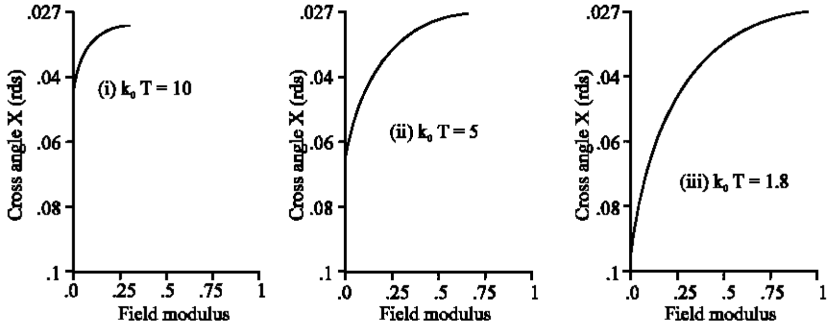

Fig. 6: Computation of the normalised cross section field in medium (n_2) versus the cross angle X. The saddle points in (i), (ii) and (iii) are located in the guided wave region. Mode 1, normalised critical thickness = 1.75, a = 0.027 rds, $n_1 = 2$, $n_2 = 1.76$, $n_3 = 1$

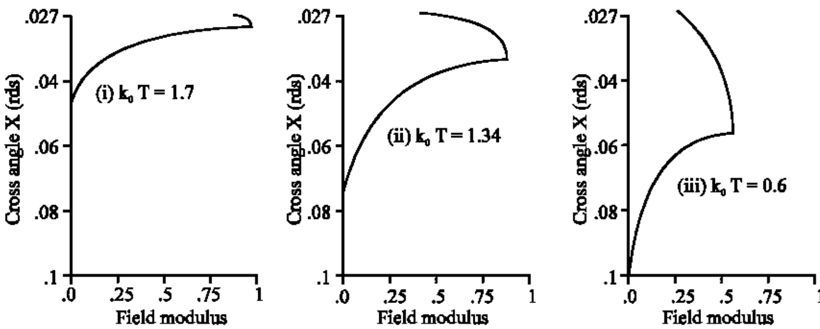

Fig. 7: Computation of the normalised cross section field in medium (n_2) versus the cross angle X. The saddle points in (i), (ii) and (iii) are located in the leaky wave region. Mode 1, normalised critical thickness = 1.75. The top of each figure represents the caustic

directionality of the beam of the radiation pattern in medium (n_2) (Belghoraf, 2001 a,b). It is the existence of this caustic that causes the field (in each diagram of Fig. 7) to oscillate in one part of the cross section pattern and decay exponentially in the other. We also notice that the amplitude of the field maximum becomes smaller as the thickness k_0 T diminishes from one diagram of Fig. 7 to another. This emphasises the fact that as θ_q moves in the leaky wave region, away from θ_c and towards $\pi/2$, the field tends to vanish. The same remarks apply to any higher mode.

REFERENCES

Arnold, J.M., A. Belghoraf and A. Dendane, 1985. Intrinsic mode theory of tapers for integrated optics, I.EEE. Proc. J. Optoelectronics, 132: 34-41.

Belghoraf, A., 1988. A computer program for the determination of the steepest descent path, applied to analysis of the tapered waveguide in integrated optics. AMSE periodicals modeling, Simulation and Control, A., 16: 7-15.

Belghoraf, A., 1992. Numerical comparaison between intrinsic and adiabatic modes for tapered optical waveguide in optical communication. A.M.S.E. periodicals, modeling. Measurement and Control, 45: 21-42.

Belghoraf, A., 2001a. A simplified approach for analysing non uniform structure in integrated optics. AMSE J. Modeling, Measurement and Control A, General Physics, 74: 61-71.

Belghoraf, A., 2001b. Numerical analysis of tapered structure in optical communication, AMSE J., Modelling Measurement and Control A, General Physics, 74: 51-60.

Oliver, F.W.J., 1974. Asymtotic and Special Function, Academic Press, N.Y.

Tamir, T., 1979. Integrated Optics', Second Updated Edition, Springler-verlag.